Green Synthesis of Surfactant Capped CTAB@Ag Nanoparticles and Study of Its Catalytic Activity

Julekha A. Shaikh (shaikhjulekha@maharashtracollege.org)
Maharashtra College of Arts, Science and Commerce https://orcid.org/0000-0003-2010-5806

Research Article

Keywords: Ginger Extract, Hydrothermal, Silver Nanoparticles, Surfactant, Catalytic Reduction

Posted Date: January 11th, 2022

DOI: https://doi.org/10.21203/rs.3.rs-1234065/v1

Abstract

In the present study, ginger extract, which is widely available as a medicinal herb, is used to develop a facile method for green synthesis of bare Ag and surfactant capped CTAB@Ag nanoparticles via Hydrothermal route. The as-prepared Ag nanoparticles were characterized by UV-Vis spectroscopy, photoluminescence (PL), X-ray Diffraction (XRD), Infrared spectroscopy (IR), and Scanning electron microscopy (SEM). The catalytic properties of as prepared bare and surfactant capped CTAB@Ag nanoparticles were also investigated in reductive degradation of Methyl Orange (MO) dye and 4-Nitrophenol (4-NP). Surfactant-capped CTAB@Ag nanoparticles exhibit superior catalytic properties in the degradation of MO and conversion of 4-nitro phenol to 4-amino phenol when compared to bare silver nanoparticles.

Article Highlights

- Bare and surfactant doped Ag nanoparticles were synthesized via green route.
- The as-prepared bare Ag and CTAB@Ag NPs were characterized by various spectroscopic techniques.
- The as-prepared bare Ag and CTAB@Ag NPs have smaller in particles size.
- The as-prepared CTAB@Ag NPs have excellent catalytic activities (3 min) for the reduction 4-nitrophenol to their 4-aminophenol and catalytic degradation of methyl orange in very short time span as compared to bare Ag NPs.

1. Introduction

The green synthesis of nanoparticles is considered as safer route due to their cost effectiveness, environmental eco-friendly nature and simplicity in control of reaction parameters [1]. Metal NPs have unique chemical and physical features, such as a large surface-to-volume ratio, that make them valuable in different sectors, including electronics, photonics, biomedicine, and catalysis [2–6]. Various types of nanomaterials such as zinc oxide, titanium oxide, gold, and silver have emerged [7] and are widely used in products that come into direct contact with the human body, such as detergents, cosmetics, tooth paste, in addition to medicinal and pharmaceutical uses [8]. Among these silver NPs have proved to be most effective as it has good antimicrobial efficacy against bacteria, viruses and other eukaryotic microorganisms. Colloidal silver is of great interest due to its unique features such as high conductivity, chemical stability, biocompatibility, and catalytic and antibacterial activity [7]. Silver nanoparticles have been regarded an essential topic of research due to their distinctive and powerful plasmon resonance in the visible region. Silver nanoparticles are used in a variety of applications, including solar energy absorption coatings and battery materials, optical receptors, chemical reaction catalysts, biolabelling, biomedical sensing and imaging, antimicrobial paint coatings, textiles, water treatment, medical equipment, HIV prevention and treatment [9–12] etc.

Traditional chemical procedures for synthesis of silver nanoparticles involve the use of ethylene glycol [13, 14], pyridine [15], and sodium borohydride [16]. However, the chemicals used in these approaches can be toxic and extremely reactive, posing a risk to the environment and individuals, or the procedures are too costly to use on a large scale. Therefore, there is a need to develop low-cost, dependable, safe, and green approach to the synthesis of stable metal nanoparticles with controlled size and form. As a result, some novel methods for the synthesis of metal nanoparticles have recently been developed using biologically derived reducing agents like chitosan [17], glucose [18], and polysaccharides [19], microbes like bacteria and fungus [20, 21] and a variety of plant (seed, leaf, and tuber) extracts [22–27]. Among them, plant leaf extract-mediated biological processes have been extensively studied due to their low cost and simple technique. During the synthesis of nanoparticles, plant extracts may act as reducing and stabilizing agents. The chemical content of the plant extract has a big impact on the size and shape of nanoparticles (NPs), which could affect their catalytic activities for degrading organic effluents [28, 29].

In the past few decades, catalysis has become the backbone of large-scale chemical and petroleum sector production. New challenges and opportunities have arisen as a result of catalysis with the advancement of nanotechnology. The nanocatalysts have a lot of catalytic activity in various reactions such as oxidation, reduction, coupling, and electrochemical reactions.

Organic contaminants present in industrial or domestic wastewater effluents must be eliminated or destroyed before being discharged into the environment. Organic dyes are one of the most common types of pollutants found in textiles, plastics, medicine, and a variety of other industries, and their hazardous effects in waste water have long been a source of concern and, more recently, a major threat to the environment. They are difficult to degrade and are rarely removed from water by wastewater treatment systems or traditional methods such as adsorption, ultrafiltration, chemical, or electrochemical approaches [30]. Therefore, a convenient degradation procedure is reductive degradation of toxic dyes using metal nanoparticles because of their unique physiochemical and electrical properties that are not present in bulk materials [31].

In this present investigation, Zingiber Officinale of the family of Zingiberaceae commonly known as ginger is used as a reducing agent for the synthesis of Ag NPs. Nanoparticles are frequently judged ineffective [32] due of their instability in aqueous medium, so in the present study surfactants are used to stabilize the NPs. A surfactant molecule is described as amphiphilic molecules that has a lengthy hydrophobic (water-hating or oil-loving) tail and a hydrophilic (water-loving) head. Depending on the type of surfactant, it greatly reduces particle size without affecting the shape [33].

The present study describes a cost-effective and environmentally friendly method for the synthesis of bare and surfactant capped silver nanoparticles using aqueous ginger root extract. Furthermore, the catalytic characteristics of these as-prepared bare and surfactant capped silver nanoparticles were investigated in the reduction of 4-nitrophenol and degradation of Methyl Orange.

2. Experimental

2.1 Materials and methods

Silver nitrate ($AgNO_3$), Cetyltrimethylammonium bromide (CTAB), Methyl orange (MO), sodium borohydride ($NaBH_4$) and 4-nitrophenol were purchased from S. D. Fine chemical Ltd. All other chemicals were of analytical grade and used without further purification. Double distilled water was used for all the experiments.

2.2 Preparation of ginger extract

The fresh ginger root (rhizome) of Zingiber officinale was purchased at a local market in Mumbai, India and washed various times in double distilled water to remove dirt. The extraction process was carried out using the direct boiling method. The rhizome was cleaned with distilled water several times. In a typical process, 30 g of thoroughly cleansed finely chopped and crushed ginger was used to make the ginger extract. Further 100 mL distilled water was added to the crushed ginger, which was then boiled for 2 h. The extract mixture was cooled to room temperature and filtered thoroughly using Whatman filter paper no. 1. The filtrate was collected and stored at 4 °C for synthesis of Ag NPs.

2.3 Synthesis of bare silver nanoparticles using ginger extract

For synthesis of bare silver NPs, hydrothermal method was preferred. In a typical synthesis, 25 mL of silver nitrate salt solution (1 mM) was mixed with 10 mL of ginger extract. The reaction mixture was refluxed with continuous stirring for 2 h. After 2 h the resultant suspension was cooled, centrifuged and washed 4 - 5 times with deionized water (DI). The centrifugate product obtained was dried in oven at 70 $^{\circ}C$ for 10 h and used for further characterizations.

2.4 Synthesis of surfactant capped silver nanoparticles using ginger extract

In a typical synthesis, 25 mL of silver nitrate salt solution (1 mM) was mixed with 10 mL of ginger extract and 10 mM (25 mL) of CTAB was added into it. The obtained solution was refluxed with continuous stirring for 2 h. The resultant suspension was cooled, centrifuged and washed 4-5 times with DI water. The obtained product was dried in an oven at 70 °C for 10 h before being used for further analysis.

2.5 Characterization of materials

The powder X-ray diffraction (XRD) patterns were carried out on a Rigaku D/MAX X-ray diffractometer, using Cu Kα radiation with λ = 0.15406 nm. Fourier transform infrared (FTIR) spectra were recorded in the range of 400-4000 cm^{-1} with Perkin Elmer FTIR spectrophotometer. The morphology of bare and surface modified silver nanoparticles were recorded using scanning electron microscopy (SEM) JEOL JSM-7600 FEG-SEM with the operating voltage of 0.01 to 30 kV. Absorbance spectra were recorded using a LAB UV-3000 Double beam Spectrophotometer UV-Vis spectrometer at room temperature whereas the photoluminescence spectra were recorded on Perkin Elmer LS 55 fluorescence spectrometer.

2.6 Catalytic activity

2.6.1 Catalytic reduction of 4-nitrophenol

The catalytic activity of bare and surfactants capped Ag NPs was determined by the reduction of 4-NP to 4-AP in the presence of $NaBH_4$. In a 100 mL beaker containing 50 mL of 4-NP solution (1 mM), 10 mL of $NaBH_4$ (10 mM) and 5 mg of catalyst, i.e., bare and surfactant capped CTAB@Ag NPs, were added. The solution was then continuously stirred with a magnetic stirrer. The 3 mL of aliquot solution was withdrawn at different time intervals and reduction reaction was monitored using UV-Visible spectroscopy.

2.6.2 Catalytic degradation of Methyl Orange

The catalytic degradation activity of bare and surfactant capped Ag NPs was determined by the degradation of methyl orange in the presence of $NaBH_4$. 50 ml of 20 ppm (20 mg/L) solution was taken from stock MO solution in a 100 mL beaker along with 10 mL of $NaBH_4$ (10 mM) and 5 mg of catalyst i.e. bare and surfactant capped CTAB@Ag NPs. A magnetic stirrer was used to mix the solution continuously. At different time intervals, 3 mL of aliquot solution was withdrawn, and the catalytic degradation reaction was monitored using UV-Visible spectroscopy.

3. Results And Discussion

3.1 X-Ray Diffraction studies

The as-prepared bare Ag and CTAB@Ag nanomaterials were characterized by XRD analysis. Figure 1 displays the XRD spectra of bare Ag and CTAB@Ag nanoparticles. It shows three distinct diffraction peaks at 38.06°, 44.21° and 64.37° corresponding to (111), (200) and (220) lattice planes, indexed as FCC silver structure (JCPDS, file no. 04-0783) [27]. Average crystallite size (D) was calculated using Scherrer's formula. The sharpness of the XRD peaks indicates that the bare Ag and CTAB@Ag nanomaterials are very crystalline in nature. The calculated crystallite size was found to be 25.6 nm for bare Ag and 28.7 nm for CTAB@Ag using the (111) diffraction peak.

$D = 0.9 \lambda / \beta \cos\theta$

Where, $\lambda = 1.54060$ Å($Cu K_{\alpha}$) and β is FWHM (in radians) at the diffraction angle.

3.2 SEM analysis

SEM was used to examine the surface morphology of as-prepared bare Ag and CTAB@Ag nanoparticles, as shown in Figure 2. The SEM analysis shows the bare and surfactant capped Ag NPs have smaller particle sizes. The SEM images exhibits a few agglomerations of bare Ag and CTAB@Ag nanoparticles with spherical and irregular morphology. The larger silver nanoparticles could be the result of aggregation of the smaller ones.

3.3 UV-Visible Studies

Noble metals are known for their unique optical properties due to the surface plasmon resonance property (SPR). The formation of silver nanoparticles was monitored using UV-Vis spectroscopy [7, 34]. Figure 3 shows the UV-Visible spectra of bare Ag and CTAB@Ag nanoparticles. The absorption spectra show the characteristics peaks located at 400-480 nm of bare Ag and CTAB@Ag nanoparticles. The broad peaks suggested the formation of various shape and size of Ag nanoparticles [35]. The optical band of bare Ag and CTAB@Ag nanoparticles were calculated using Tauc's plot [36].

$\alpha h\upsilon = A\,(h\upsilon - E_g)^{n/2}$ (1)

Where A is the proportionality constant, α is the absorption coefficient, h is the plank constant, υ is the frequency of incident photons, hυ is the energy of absorption and E_g is optical band gap (separation between valence band and conduction bands) and the component n depends on the optical transition. For the direct band n = 1 and indirect band gap n = ½ [36]. The E_g value of optical band gap of bare Ag and CTAB@Ag was calculated by extra plotting a linear graph of $(\alpha h\upsilon)^2$ vs. photon energy (hυ) were found to be 2.55 eV and 2.48 eV, respectively (Figure 4).

3.4 Photoluminescence (PL) studies

Figure 5 show the fluorescence spectra of bare Ag and CTAB@Ag nanoparticles obtained with 380 nm excitation wavelength. The PL spectra show the emission peak of bare Ag and CTAB@Ag nanoparticles at 468 nm and 469 nm, respectively [1]. The PL intensity of CTAB@Ag is lower as compared to bare Ag nanoparticles, which indicating the CTAB@Ag has higher electron-hole pair separation efficiency.

3.5 FTIR analysis

In the present study, FTIR spectra are used to identify biomolecules that are responsible for capping and stabilizing silver nanoparticles. FTIR spectra of bare Ag and CTAB@Ag are shown in Figure 6. The strong bands observed at 3256 cm^{-1} and 3276 cm^{-1} are due to presence of –OH stretching vibration in both bare Ag and CTAB@Ag nanoparticles, respectively. The medium intensity stretching bands observed at 2924 cm^{-1} in bare Ag and 2918 cm^{-1}, 2843 cm^{-1} in case of CTAB@Ag nanoparticles is due to presence of –CH stretching band of hydrocarbon [37]. The strong bands observed at 1631 cm^{-1} and 1624 cm^{-1} in bare Ag and CTAB@Ag nanoparticles respectively suggests the presence of stretching vibration of –C=C (alkene) [38]. Strong and medium intensity bands are observed in bare Ag and CTAB@Ag at 1444-1473 cm^{-1}, 1348-1361 cm^{-1}, 1152-1183 cm^{-1} attributed due to presence of methyl group, ether, alcohol. Some others bands at 996-1017 cm^{-1}, 754-760 cm^{-1} and 567-608 cm^{-1} are significant indicators of heterocyclic chemicals such as flavonoids and alkaloids, which are active components of Z. officinale and serve as a capping agent [35, 37, 38].

3.6 Catalytic activity

3.61 Catalytic reduction of 4-nitrophenol

The catalytic activity of bare Ag NPs and CTAB@Ag were investigated for reduction of 4-nitrophenol to 4-aminophenol using $NaBH_4$ as shown in Figure 7. The maximum absorption of 4-NP in aqueous solution is 317 nm, but when $NaBH_4$ is added, the peak shifts to 400 nm due to the formation of 4-nitrophenolate ion. The UV–Vis spectral method was used to monitor the catalytic reduction activity. Figure 7 **(a)** shows the presence of bare Ag NPs even after 45 minutes which indicates that the reduction of (4-NP) to (4-AP) does not occur. The nitro compound could not be degraded by $NaBH_4$ alone, and Ag NPs did not demonstrate efficient degradation, indicating that neither $NaBH_4$ nor Ag NPs are capable of catalyzing the fast reduction of 4-nitrophenol to 4-amonophenol. Furthermore, when the surfactant capped CTAB@Ag nanoparticles was used, the reduction rate increases, indicating that CTAB@Ag act as a catalyst in the reduction of 4-nitrophenol. After the addition of surfactant capped i.e. CTAB@Ag NPs, the red shift region at 400 nm dropped out and new peak shoulder at 298 nm appeared simultaneously, confirming the reduction of a 4-nitrophenolate ion to 4-aminophenol. Figure 7 **(b)** shows that in the presence of CTAB@Ag NPs the reduction reaction is completed within 3 min. In conclusion, surfactant capped Ag NPs shows excellent catalytic activity as compared to bare Ag NPs. The Langmuir-Hinshelhood equation [39] was used for calculation of reduction efficiency rate constant (k) of catalyst based on $\ln(C/C_0) = kt$, where k is rate constant and t represent reduction time. Figure 8 **(a)** show the plot of C/C_0 vs time and Figure 8 **(b)** show plot of $\ln(C/C_0)$ vs time. The linear plot of $\ln(C/C_0)$ vs time revealed that the rate of reduction reaction kinetics is pseudo-first-order. The efficiency of reduction rate constant value of CTAB@Ag is 1.016 min^{-1}, which is higher that bare Ag (0.035 min^{-1}). This result confirms that surfactant caped i.e. CTAB@Ag exhibits better catalytic performance as compared to bare Ag NPs. Furthermore, the as-prepared CTAB@Ag catalyst is superior as compared previously reported Ag catalysts for reduction of nitro aromatic compounds (as shown in Table 1).

Table 1
Comparative catalytic reduction of nitro compounds by various catalysts.

Catalysts	Nitro compounds	Time (min)	References
Ag NPs	4-NP	15	40
Ag NPs	4-NP	15	41
Ag NPs	4-NP	12	42
Ag NPs	4-NP	22	43
Ag NPs	4-NP	24	44
Ag NPs	4-NP	12	45
CTAB@Ag	**4-NP**	**3**	**This work**

3.6.2 Catalytic degradation of Methyl Orange (MO)

The degradation of an azo dye Methyl Orange in the presence of bare Ag and surfactant capped CTAB@Ag nanoparticles are shown in Figure 9. The maximum absorption of MO is known to appear at 465 nm. The blank experiment was performed without the catalyst and it was observed that the absorption intensity decreases slightly on the addition of $NaBH_4$, but the colour of MO solutions does not change. On addition of bare Ag NPs along with $NaBH_4$, the MO solution absorption intensity does not diminish completely even after 20 min as shown in Figure 9 **(a)**. Furthermore, the absorption intensity decreases drastically after adding of small amount of surfactant caped i.e. CTAB@Ag catalyst and it completely disappears after 3 minutes. Figure 9 **(b)** show the decrease of absorption intensity of MO at different time intervals in present of CTAB@Ag catalyst. The rate constant value of catalytic degradation of MO in presence of bare Ag and CTAB@Ag were calculated using Langmuir-Hinshelhood equation [39]. Figure 10 (a and b) show the plot of C/C_0 vs. time and $\ln(C/C_0)$ vs. time for bare Ag and CTAB@Ag catalysts. Figure 10 **(b)** show a linear plot, which demonstrates that the rate of reaction for the degradation of dye is pseudo-first-order kinetic reaction. The rate constant (k) values are calculated 0.7904 min^{-1} (CTAB@Ag) and 0.0607 min^{-1} (bare Ag) from the slopes of $\ln(C/C_0)$. From the slope it was observed that surfactant capped catalyst has excellent catalytic activity as compared to bare Ag catalyst for the degradation of MO dye. In addition, when compared to previously reported Ag catalysts for the catalytic degradation of methyl orange, the as-prepared CTAB@Ag catalyst is superior (as shown in Table 2).

Table 2
Comparative catalytic degradation of methyl orange using different catalysts.

Catalyst	Methyl Orange	Time (min)	References
Ag NPs	MO	13	46
Ag NPs	MO	6	47
Ag NPs	MO	45	48
Ag NPs	MO	6	49
Ag NPs	MO	45	50
Ag NPs	MO	10	51
Ag NPs	MO	11	52
CTAB@Ag	**MO**	**3**	**This work**

4. Conclusion

In the conclusion, synthesis of bare and surfactant capped silver nanoparticles from greener route using Ginger extract. Surfactant is utilised to keep the silver nanoparticles stable. When compared to bare silver nanoparticles, surfactant capped CTAB@Ag nanoparticles have smaller particle sizes. Further, all synthesized nanoparticles were used a catalyst for the reduction 4-nitrophenol and deradation of Methyl Orange. Thus, the surfactant capped nanoparticles (CTAB@Ag), were shown to have excellent catalytic activity for the reduction of 4-nitrophenol to 4-amino phenol and degradation of methyl orange dye in presence of $NaBH_4$ as reducing agent as compared to bare Ag NPs. The as-synthesized surfactant capped CATB@Ag are able to convert 4-nitrophenol to 4-aminophneno and degrade the MO within 3 minutes, respectively. The as-prepared surfactant capped CTAB@Ag nanoparticles are the most promising catalysts, with good potential use as a catalyst in organic reactions and in the purification of industrial waste water, among other applications.

Declarations

Declaration of Competing Interest

The author declares that there are no financial or commercial conflicts of interest that could have appeared to influence the work stated in this paper.

Acknowledgement

The author is thankful to University of Mumbai, India for providing research analysis facility and also acknowledge SAIF IIT Bombay for providing SEM images.

References

1. S. Ahmed, M. Saifullah, Ahmed, B.L. Swami, S. Ikram, Green synthesis of silver nanoparticles using Azadirachta indica aqueous leaf extract. J Radiat Res Appl Sci **9**, 1–7 (2016)
2. M.C. Daniel, D. Astruc, Gold Nanoparticles: Assembly, Supramolecular Chemistry, Quantum-Size-Related Properties, and Applications toward Biology, Catalysis, and Nanotechnology. Chem. Rev. **104**, 293–346 (2004)
3. S.A. Maier, M.L. Brongersma, P.G. Kik, S. Meltzer, A.A.G. Requicha, H.A. Atwater, Plasmonics-A Route to Nanoscale Optical Devices. Adv Mater **13**, 1501–1505 (2001)
4. C.A. Mirkin, R.L. Letsinger, R.C. Mucic, J.J. Storhoff, A DNA-based method for rationally assembling nanoparticles into macroscopic materials. Nature **382**, 607–610 (1996)
5. H. Tsunoyama, H. Sakurai, N. Lchikuni, Y. Negish, T. Tsukuda, Colloidal Gold Nanoparticles as Catalyst for Carbon–Carbon Bond Formation: Application to Aerobic Homocoupling of Phenylboronic Acid in Water. Langmuir **20**, 11293–11296 (2004)
6. J. Saha, B. Arjuara, M. Avik, S. Kumar, A novel green synthesis of silver nanoparticles and their catalytic action in reduction of Methylene Blue dye. Sustain Environ Res **27**, 245–250 (2017)
7. P. Logeswari, S. Silambarasan, J. Abraham, Synthesis of silver nanoparticles using plants extract and analysis of their antimicrobial property. J Saudi Chem Soc **19**, 311–317 (2015)
8. G. Parthasarathy, M. Saroja, M. Venkatachalam, P. Gowthaman, V.K. Evanjelene, Synthesis of Nano Particles From Aloe Vera Extract – Review Paper. Imp J Interdiscip Res **2**, 1570–1575 (2016)
9. K. Anandalakshmi, J. Venugobal, V. Ramasamy, Characterization of silver nanoparticles by green synthesis method using Pedalium murex leaf extract and their antibacterial activity. Appl Nanosci **6**, 399–408 (2016)
10. A. Kumar, P.K. Vemula, P.M. Ajayan, G. John, Silver-nanoparticle-embedded antimicrobial paints based on vegetable oil. Nature **7**, 236–241 (2008)
11. R.A. Khaydarov, R.R. Khaydarov, O. Gapurova, Y. Estrin, T. Scheper, Electrochemical method for the synthesis of silver nanoparticles. J. Nanopart. Res. **11**, 1193–1200 (2008)
12. C.J. Murphy, A.M. Gole, S.E. Hunyadi, J.W. Stone, P.N. Sisco, A. Alkilany, B.E. Kinard, P. Hankins, Chemical sensing and imaging with metallic nanorods. Chem. Commun. **5**, 544–557 (2008)
13. Y. Sun, B. Gates, B. Mayers, Y. Xia, Crystalline Silver Nanowires by Soft Solution Processing. Nano Lett. **2**, 165–168 (2002)
14. B. Wiley, T. Herricks, Y. Sun, Y. Xia, Polyol Synthesis of Silver Nanoparticles: Use of Chloride and Oxygen to Promote the Formation of Single-Crystal, Truncated Cubes and Tetrahedrons. Nano Lett. **4**, 1733–1739 (2004)
15. J.A. Creighton, C.G. Blatchford, M.G. Albrecht, Plasma resonance enhancement of Raman scattering by pyridine adsorbed on silver or gold sol particles of size comparable to the excitation wavelength. J Chem Sot Faraday II **75**, 790–798 (1979)

16. J.S. Kim, E. Kuk, K.N. Yu, J.H. Kim, S.J. Park, H.J. Lee, S.H. Kim, Y.K. Park, Y.H. Park, C.Y. Hwang, Y.K. Kim, Y.S. Lee, D.H. Jeong, M.H. Cho (2007) Antimicrobial effects of silver nanoparticles. Nanomed: Nanotechnol Biol Med 3:95-101
17. N.M. Huang, S. Radiman, H.N. Lim, P.S. Khiew, W.S. Chiu, K.H. Lee, A. Syahida, R. Hashim, C.H. Chia, γ-Ray assisted synthesis of silver nanoparticles in chitosan solution and the antibacterial properties. Chem. Eng. J. **155**, 499–507 (2009)
18. A.T. Le, P.T. Huy, P.D. Tam, T.Q. Huy, P.D. Cam, A.A. Kudrinskiy, Y.A. Krutyakov, Green synthesis of finely-dispersed highly bactericidal silver nanoparticles via modified Tollens technique. Curr. Appl. Phys. **10**, 910–916 (2010)
19. T.C.Y. Leung, C.K. Wong, Y. Xie, Green synthesis of silver nanoparticles using biopolymers, carboxymethylated-curdlan and fucoidan. Mater Chem Phys **121**, 402–405 (2010)
20. M. Saravanan, A. Nanda, Extracellular synthesis of silver bionanoparticles from Aspergillus clavatus and its antimicrobial activity against MRS A and MRSE. Colloid Surface B **77**, 214–218 (2010)
21. L. Sintubin, W.D. Windt, J. Dick, J. Mast, D. Van der Ha, W. Verstraete, N. Boon, Lactic acid bacteria as reducing and capping agent for the fast and efficient production of silver nanoparticles. Appl Microbiol Biot **84**, 741–749 (2009)
22. R. Sanghi, V. Preeti, pH dependant fungal proteins in the 'green' synthesis of gold nanoparticles. Adv Mat Lett **1**(3), 193–199 (2007)
23. A.R. Shahverdi, S. Minaeian, H.R. Shahverdi, H. Jamalifar, A.A. Nohi, Rapid synthesis of silver nanoparticles using culture supernatants of Enterobacteria: A novel biological approach. Pro Biochem 42:919–923
24. S.S. Shankar, A. Ahmad, M. Sastry, Geranium Leaf Assisted Biosynthesis of Silver Nanoparticles. Biotechnol Prog **19**, 1627–1631 (2003)
25. S.S. Shankar, A. Rai, A. Ahmad, M. Sastry, Rapid synthesis of Au, Ag, and bimetallic Au core–Ag shell nanoparticles using Neem (Azadirachta indica) leaf broth. J Colloid Interf Sci **275**, 496–502 (2004)
26. B. Ankamwar, M. Chaudhary, M. Sastry, Gold Nanotriangles Biologically Synthesized using Tamarind Leaf Extract and Potential Application in Vapor Sensing. Synth React Inorg Met Org Chem **35**, 19–26 (2005)
27. M.N. Nadagouda, R.S. Varma, Green synthesis of silver and palladium nanoparticles at room temperature using coffee and tea extract. Green Chem. **10**, 859–862 (2008)
28. V. Kumar, S.K. Yadav, Plant-mediated synthesis of silver and gold nanoparticles and their applications. J. Chem. Technol. Biotechnol. **84**, 151–157 (2009)
29. A.K. Mittal, Y. Chisti, U.C. Banerjee, Synthesis of metallic nanoparticles using plant extracts. Biotechnol. Adv. **31**, 346–356 (2013)
30. S. Bhakya, S. Muthukrishnan, M. Sukumaran, M. Muthukumar, K.T. Senthil, M.V. Rao, Catalytic Degradation of Organic Dyes using Synthesized Silver Nanoparticles: A Green Approach. J Bioremediat Biodegrad **6**, 1000312 (2015)

31. K. Jyoti, A. Singh, Green synthesis of nanostructured silver particles and their catalytic application in dye degradation. J Genetic Eng Biotech **14**, 311–317 (2016)
32. A. Das, R. Chadha, N. Maiti, S. Kapoor, Role of Surfactant in the Formation of Gold Nanoparticles in Aqueous Medium. J Nanopart Res 2014:1–7
33. S. Hussain, S. Ahmed, K. Al-Thabaiti, Zaheer, Surfactant-assisted bio-conjugated synthesis of silver nanoparticles (AgNPs). Bioprocess. Biosyst. Eng. **37**, 1727–1735 (2014)
34. H. Veisi, S. Azizi, P. Mohammadi, Green synthesis of the silver nanoparticles mediated by Thymbra spicata extract and its application as a heterogeneous and recyclable nanocatalyst for catalytic reduction of a variety of dyes in water. J Cleaner Prod **170**, 1536–1543 (2018)
35. K. Barman, D. Chowdhury, P.K. Baruah, Bio-synthesized silver nanoparticles using Zingiber officinale rhizome extract as efficient catalyst for the degradation of environmental pollutants. Inorg Nano-Met Chem **50**, 57–65 (2020)
36. Y. Yang, J. Liang, W. Jin, Y. Li, M. Xuan, S. Wang, X. Sun, C. Chen, J. Zhang, The design and growth of peanut-like CuS/$BiVO_4$ composites for photoelectrochemical sensing. RSC Adv **10**, 14670–14678 (2020)
37. X. Zhai, Y. Xia, D. Sun, J. Xu, Cd^{2+} Counterion-Assisted Synthesis of Uniform CdS Nanospheres Capped with the Anionic Surfactant Sodium dodecylsulfate. J Dispersion Sci Tech **35**, 76–83 (2014)
38. M. Raafat, A.S.A. El-Sayed, M.T. El-Sayed, Biosynthesis and Anti-Mycotoxigenic Activity of Zingiber officinale Roscoe-Derived Metal Nanoparticles. Molecules **26**, 2290 (2021)
39. I.K. Konstantinou, T.A. Albanis, TiO_2-assisted photocatalytic degradation of azo dyes in aqueous solution: kinetic and mechanistic investigations: A review. Appl Catal B Enviorn **49**, 1–14 (2004)
40. G. Dinda, D. Halder, A. Mitra, N. Pal, D.K. Chattoraj, Phytosynthesis of silver nanoparticles using Zingiber officinale extract: evaluation of their catalytic and antibacterial activities. J Dispers Sci Technol **41**, 2128–2135 (2020)
41. W.H. Eisa, M.F. Zayed, B. Anis, L.M. Abbas, S.S.M. Ali, A.M. Mostafa, Clean production of powdery silver nanoparticles using Zingiber officinale: The structural and catalytic properties. J Clean Prod **241**, 118398 (2019)
42. R. Begum, G. Ahmad, J. Najeeb, W. Wu, A. Irfan, M. Azam, J. Nisar, Z.H. Farooqi, Stabilization of silver nanoparticles in crosslinked polymer colloids through chelation for catalytic degradation of p-nitroaniline in aqueous medium. Chem. Phys. Lett. **763**, 138263 (2021)
43. N. Kumar, R. Bogireddy, H. Anand, K. Kumar, B.K. Mandal, Biofabricated silver nanoparticles as green catalyst in the degradation of different textile dyes. J Environ Chem Eng **4**, 56–64 (2016)
44. J. Xiong, Y. Wang, Q. Xue, X. Wu, Synthesis of highly stable dispersions of nanosized copper particles using l-ascorbic acid. Green Chem. **13**, 900–904 (2011)
45. K. Yoosaf, B.I. Ipe, C.H. Suresh, K.G. Thomas, In Situ Synthesis of Metal Nanoparticles and Selective Naked-Eye Detection of Lead Ions from Aqueous Media. J. Phys. Chem. C **111**, 12839–12847 (2007)

46. M. Ismail, M.I. Khan, M.A. Khan, K. Akhtar, A.M. Asiri, S.B. Khan, Plant-supported silver nanoparticles: Efficient, economically viable and easily recoverable catalyst for the reduction of organic pollutants. Appl Organometal Chem **33**, 4971 (2019)
47. V.K. Vidhu, D. Philip, Catalytic degradation of organic dyes using biosynthesized silver nanoparticles. Micron **56**, 54–62 (2014)
48. T. Varadavenkatesan, R. Selvaraj, R. Vinayagam, Phyto-synthesis of silver nanoparticles from Mussaenda erythrophylla leaf extract and their application in catalytic degradation of methyl orange dye. J. Mol. Liq. **221**, 1063–1070 (2016)
49. S. Iqbal, C. Zahoor, S. Musaddiq, M. Hussain, R. Begum, A. Irfan, M. Azam, Z.H. Farooqi, Silver nanoparticles stabilized in polymer hydrogels for catalytic degradation of azo dyes. Ecotoxicol. Environ. Saf. **202**, 110924 (2020)
50. U. Amjad, L. Sherin, M.F. Zafar, M. Mustafa, Comparative Study on the Catalytic Degradation of Methyl Orange by Silver Nanoparticles Synthesized by Solution Combustion and Green Synthesis Method. Arab J Sci Eng **44**, 9851–9857 (2019)
51. N. Cyril, J.B. George, L. Joseph, V.P. Sylas, Catalytic Degradation of Methyl Orange and Selective Sensing of Mercury Ion in Aqueous Solutions Using Green Synthesized Silver Nanoparticles from the Seeds of Derris trifoliate. J Clust Sci **30**, 459–468 (2019)
52. S. Joseph, B. Mathew, Microwave-assisted green synthesis of silver nanoparticles and the study on catalytic activity in the degradation of dyes. J. Mol. Liq. **204**, 184–191 (2015)

Figures

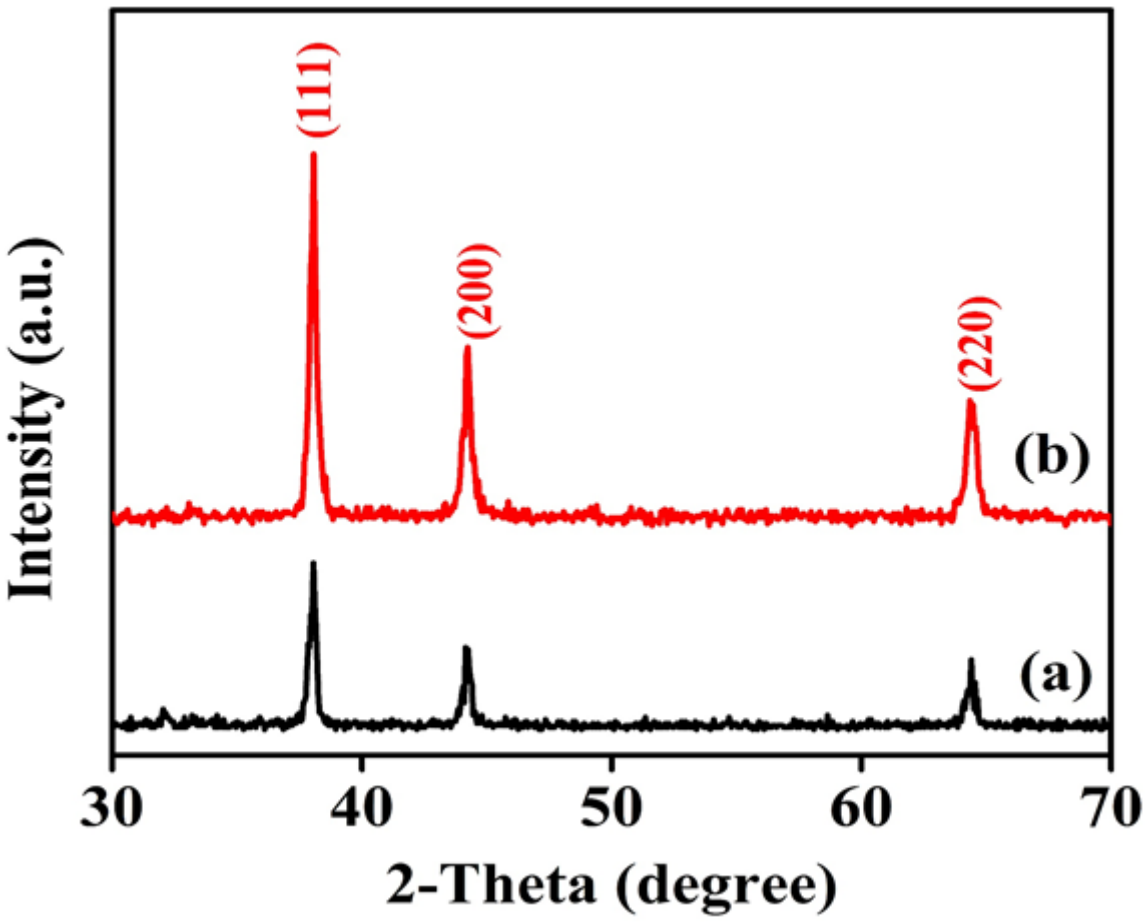

Figure 1

XRD pattern of (a) bare Ag nanoparticles and (b) CTAB@Ag nanoparticles using powder samples from 20° to 80° 2θ range at scan rate of 2-degree min^{-1}.

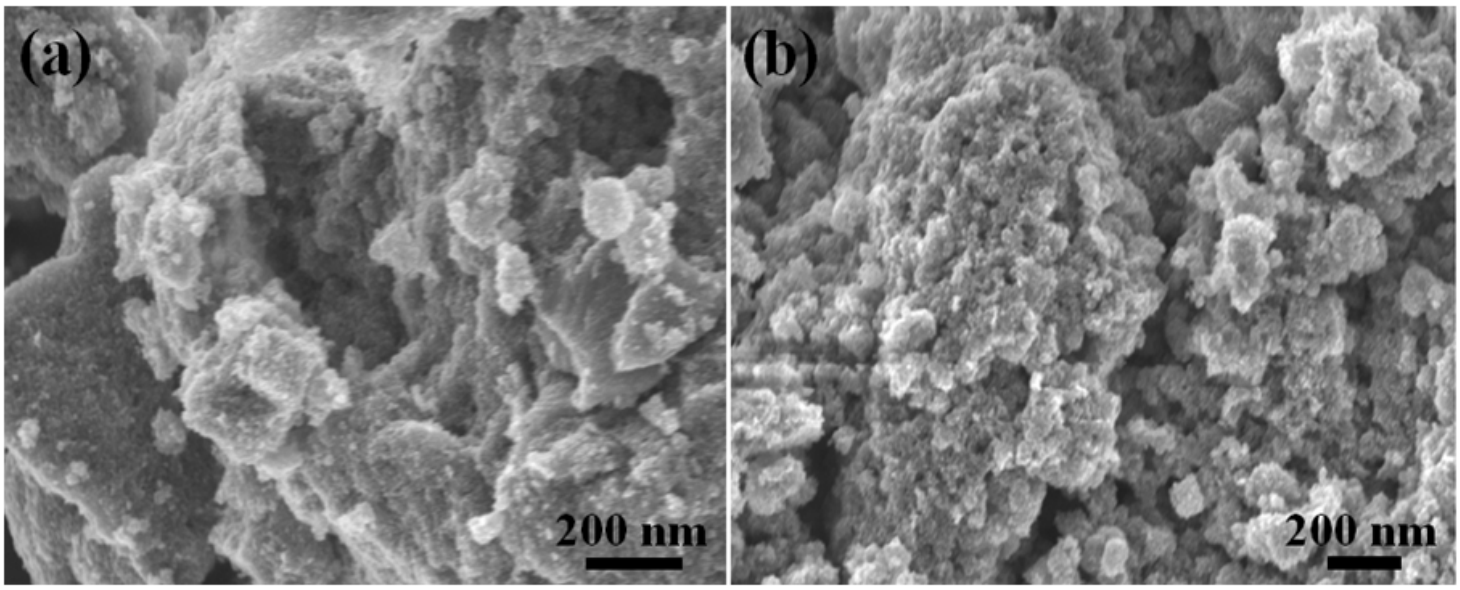

Figure 2

SEM images of (a) bare Ag nanoparticles and (b) CTAB@Ag nanoparticles using a pinch of catalyst dispersed in isopropyl alcohol and drop cast on pre-cleaned silicon wafer and air-drying.

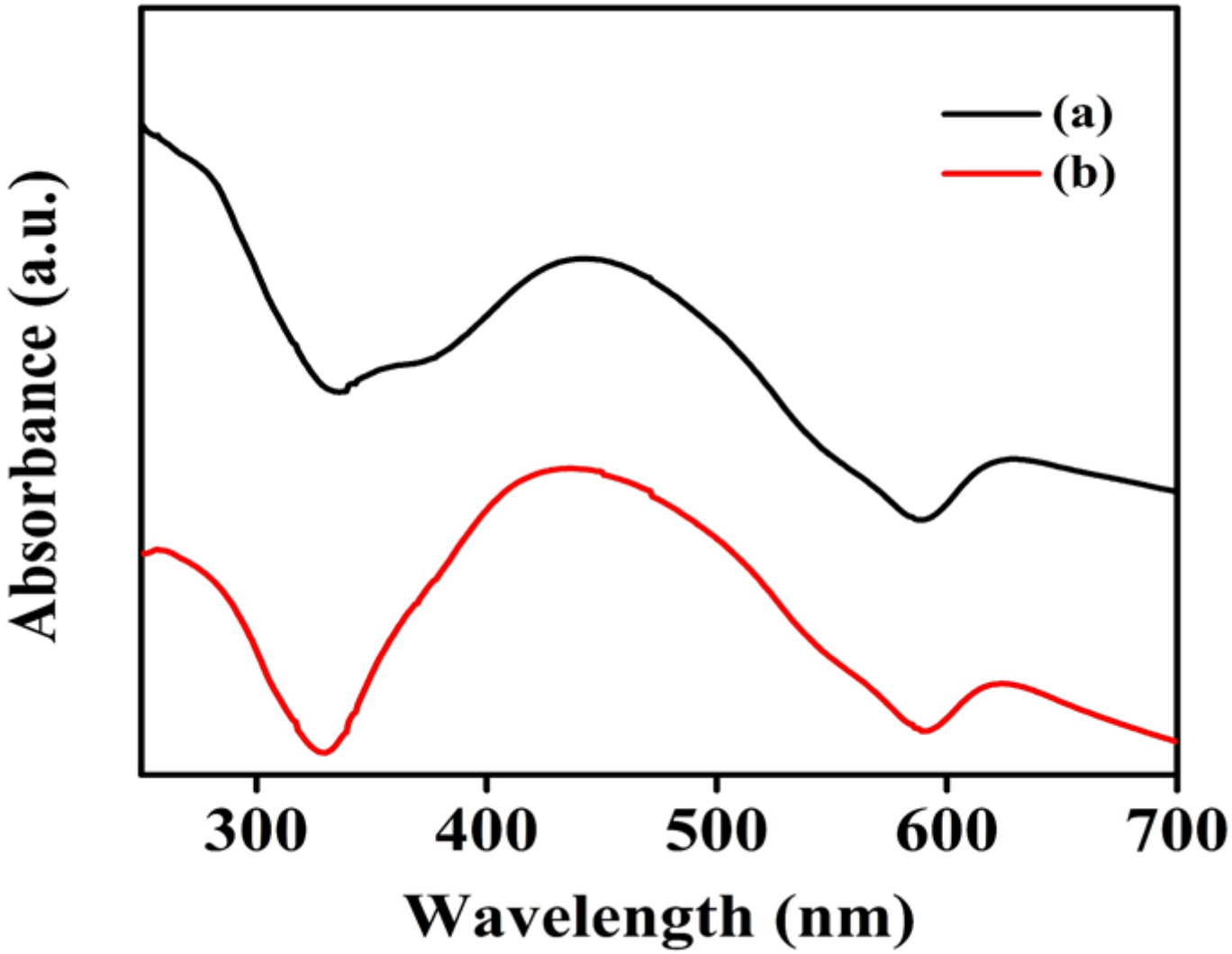

Figure 3

UV – Visible absorbance spectra of (a) bare Ag nanoparticles and (b) CTAB@Ag nanoparticles using a powder samples and dispersed in methanol.

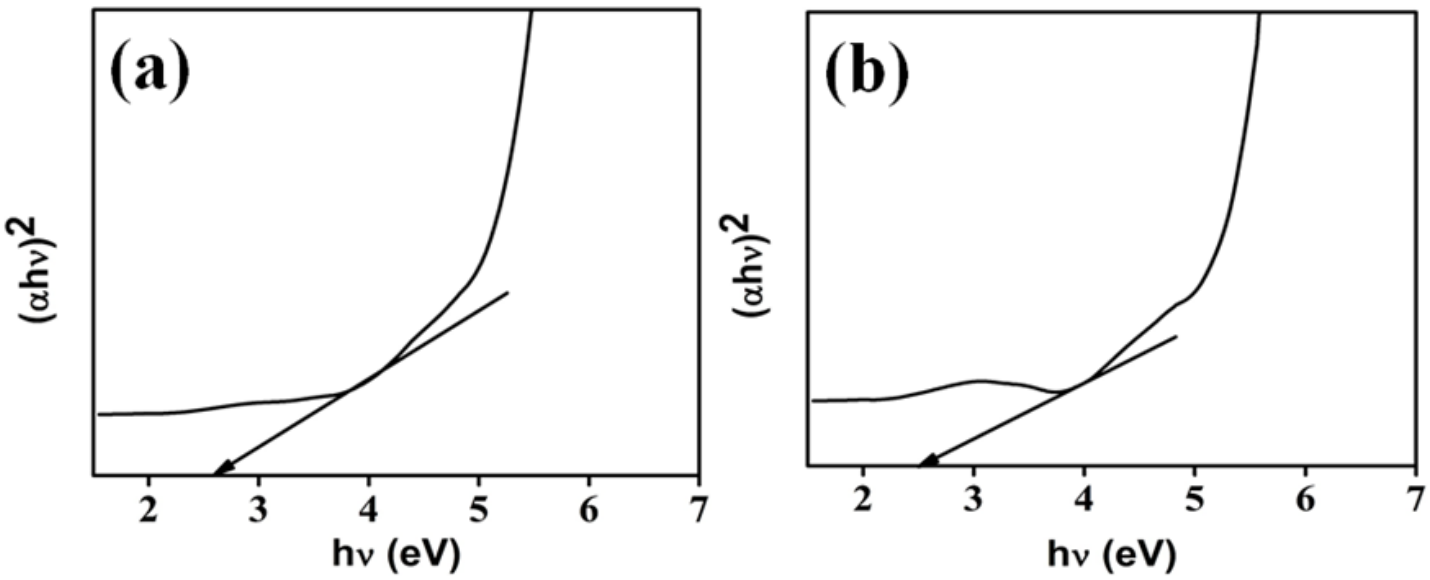

Figure 4

Tauc plots of (a) bare Ag nanoparticles and (b) CTAB@Ag nanoparticles.

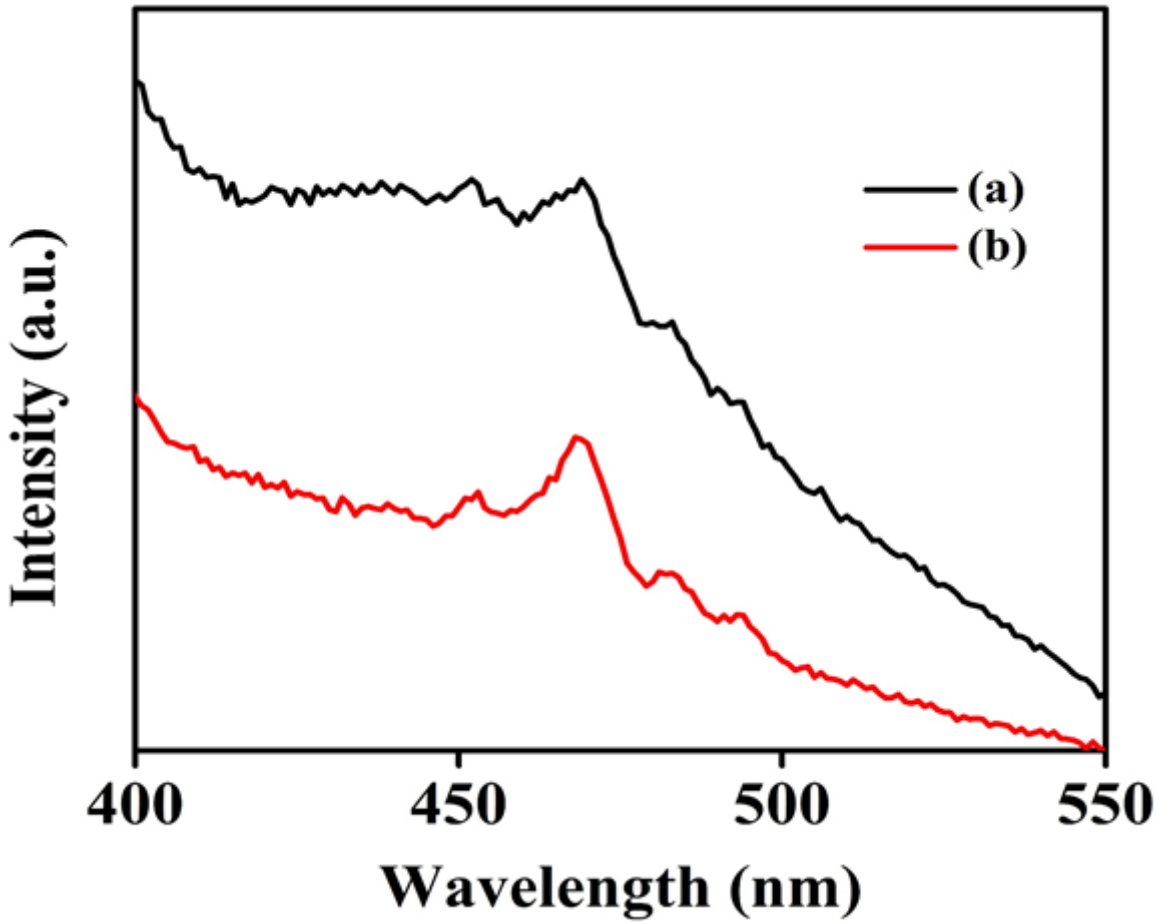

Figure 5

Photoluminescence spectra of (a) bare Ag nanoparticles and (b) CTAB@Ag nanoparticles using a powder samples and dispersed in methanol.

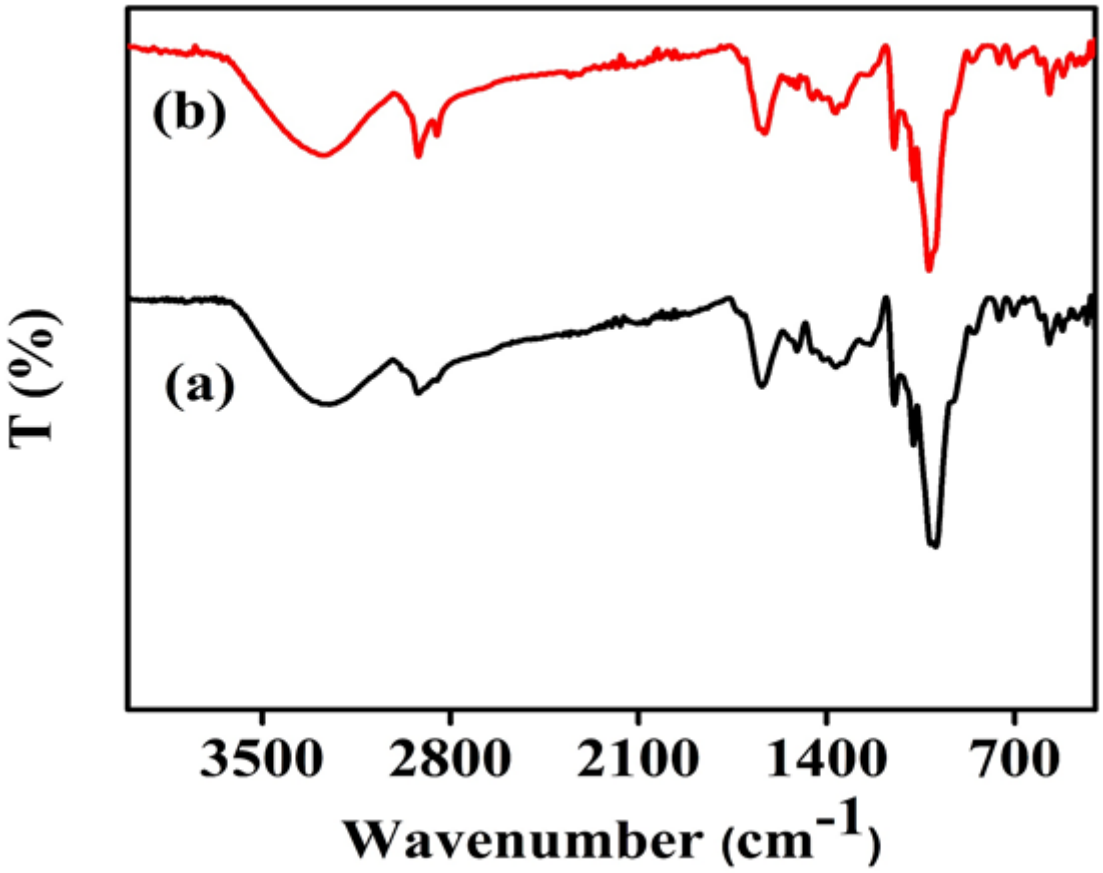

Figure 6

FTIR spectra of (a) bare Ag nanoparticles and (b) CTAB@Ag nanoparticles using a powder sample.

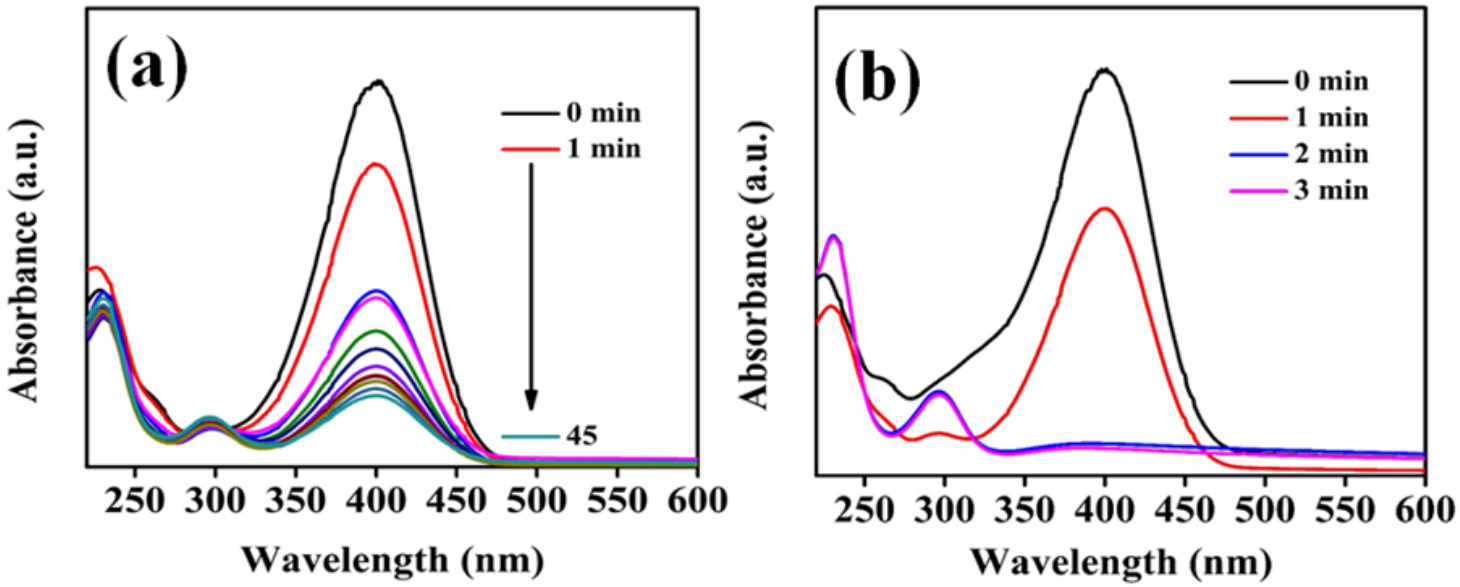

Figure 7

UV-Visible absorbance spectra for the reduction of 4-NP in the presence of (a) bare Ag and (b) CTAB@Ag catalysts.

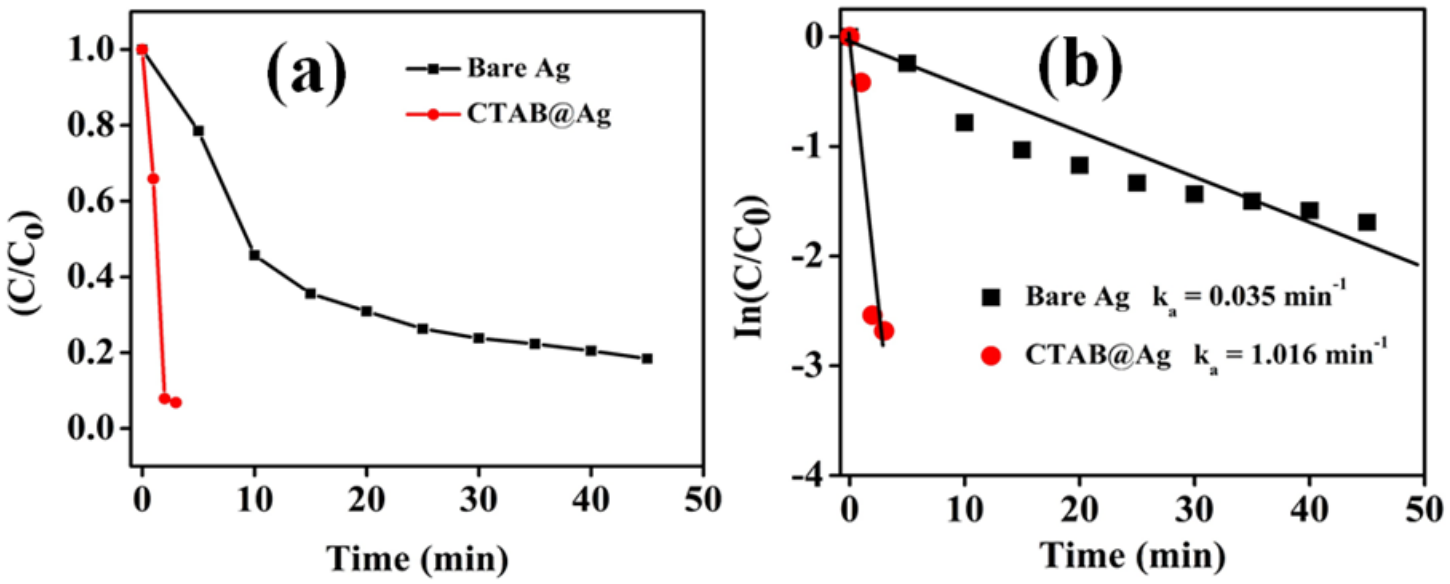

Figure 8

(a) Plot of C/C_0 vs. time and (b) $\ln(C/C_0)$ vs. time of kinetic linear fitting of the catalytic reduction of 4-NP in the presence of bare Ag and CTAB@Ag catalysts.

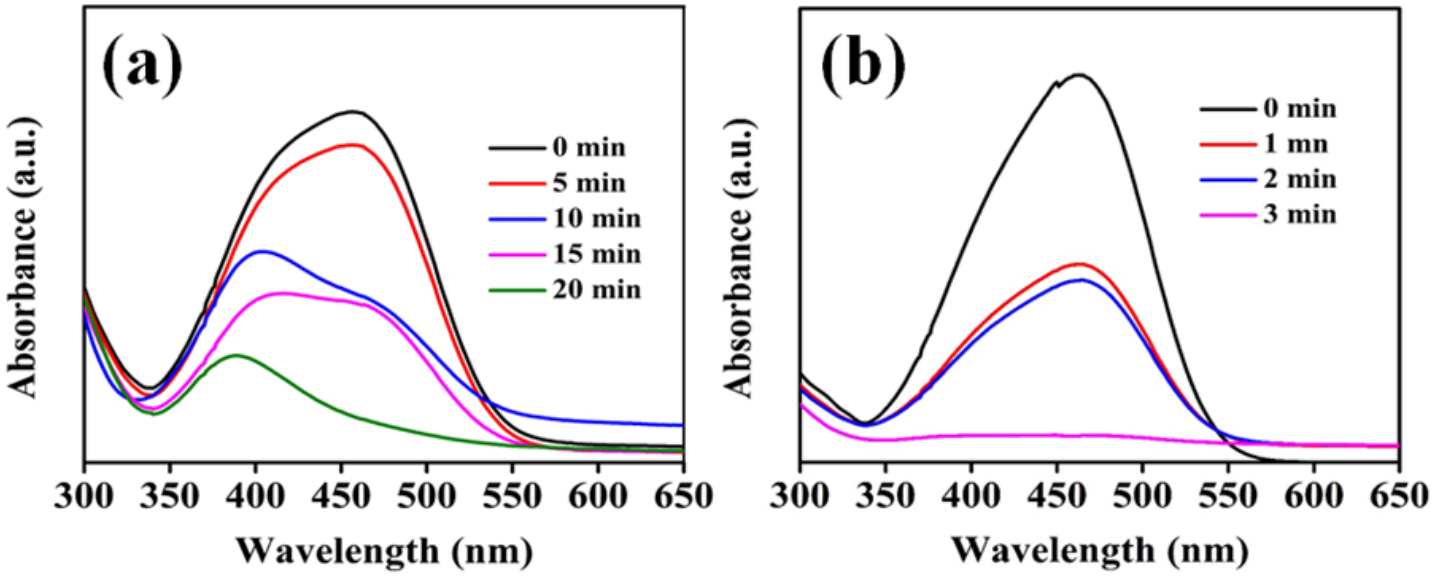

Figure 9

UV-Visible absorbance spectra for the catalytic degradation of MO in the presence of (a) bare Ag and (b) CTAB@Ag catalysts.

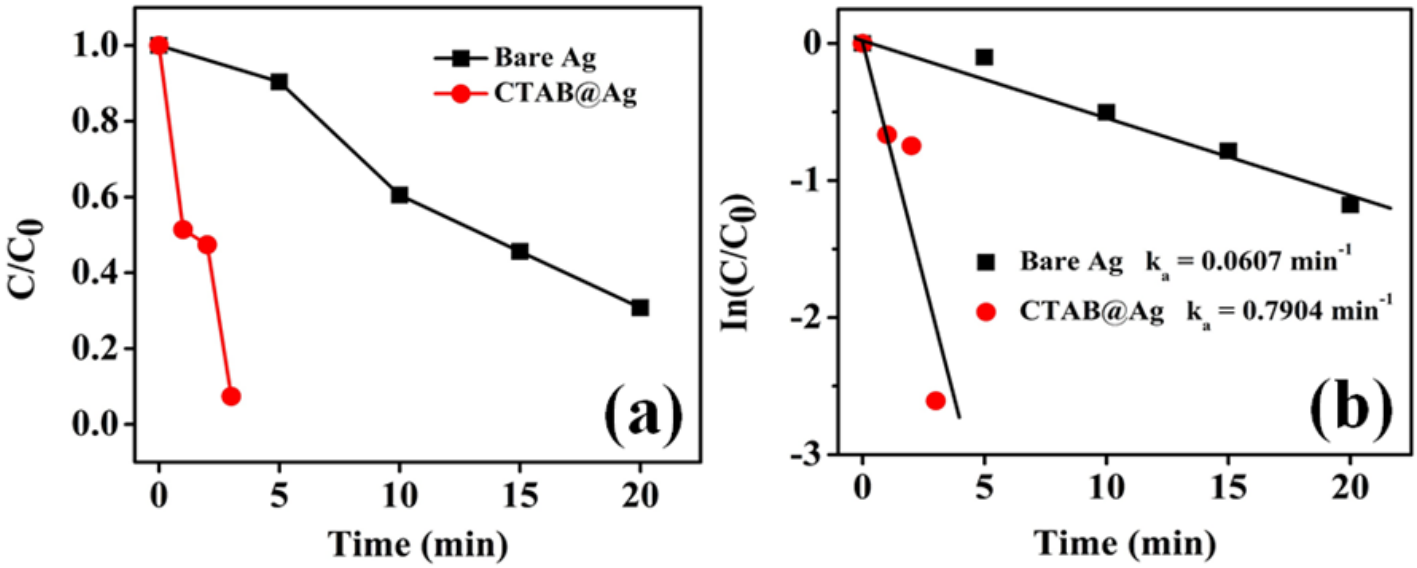

Figure 10

(a) Plot of C/C_0 vs. time and (b) $\ln(C/C_0)$ vs. time of kinetic linear fitting of the catalytic degradation of MO in presence of bare Ag and CTAB@Ag catalysts.

Supplementary Files

This is a list of supplementary files associated with this preprint. Click to download.

- GrpahicalAbstract.png